JACS
JOURNAL OF THE AMERICAN CHEMICAL SOCIETY
pubs.acs.org/JACS
Communication

Aryl Acid-Alcohol Cross-Coupling: C(sp^3)–C(sp^2) Bond Formation from Nontraditional Precursors

Eva Lin, Johnny Z. Wang, Edna Mao, Stephanie Tsang, Kurtis M. Carsch, Cesar N. Prieto Kullmer, Ryan E. McNamee, Jeffrey R. Long,* Chi "Chip" Le,* and David W.C. MacMillan*

Cite This: J. Am. Chem. Soc. 2025, 147, 14905–14914
Read Online

ACCESS | Metrics & More | Article Recommendations | Supporting Information

ABSTRACT: Alcohols and aryl carboxylic acids are among the most commercially abundant, synthetically versatile, and operationally convenient building blocks in organic chemistry. Despite their widespread availability, the direct formation of C(sp^3)–C(sp^2) bonds from these functional groups remains a challenge. Recently, our group developed robust protocols to harness alcohols as alkyl radical precursors, but the activation of aryl acids remains relatively unexplored. Herein, we describe the merger of N-heterocyclic carbene (NHC)-mediated deoxygenation and nickel-mediated decarbonylation of aryl acids toward C(sp^3)–C(sp^2) bond formation. The utility of this method is demonstrated through the synthesis of a diverse range of aryl–alkyl cross-coupled products and the late-stage functionalization of complex molecules, including drugs, natural products, and biomolecules.

Downloaded via PRINCETON UNIV on June 30, 2025 at 21:35:48 (UTC).
See https://pubs.acs.org/sharingguidelines for options on how to legitimately share published articles.

The development of new methods to form carbon–carbon bonds has the potential to greatly expand access to a valuable chemical space. Of particular importance is the C(sp^3)–C(sp^2) substructure, which plays a critical role in drug discovery and design by imparting three-dimensional complexity through C(sp^3)–rich scaffolds. These scaffolds confer improved solubility, bioavailability, and pharmacokinetic profiles and are thus highly desirable in pharmaceuticals.[1] The growing interest in incorporating sp^3-rich fragments has led to a major focus on efficient methods for constructing these linkages.[2] While sp^2 moieties remain essential for interactions such as π–π and π–cationic binding,[3] the increasing demand for C(sp^3)–rich architectures is driving synthetic innovation. Despite the importance of these scaffolds, few methods exist for their construction.[4] Methods that forge C(sp^3)–C(sp^2) bonds from readily accessible starting materials offer a powerful platform for expanding the chemical diversity and driving new discoveries.

Traditionally, the synthesis of C(sp^3)–C(sp^2) bonds has relied on cross-coupling methods involving transition metals such as palladium[5−9] paired with alkyl and aryl organometallic reagents and halides.[10−12] While these strategies have proven invaluable,[13−18] their dependence on costly or less accessible starting materials and catalysts limits their broader applications. Recent developments in nickel catalysis have opened new avenues for reductive C(sp^3)–C(sp^2) couplings,[19,20] providing complementary approaches to palladium-catalyzed methods and enabling broader substrate scope under milder conditions.

Despite these advances, existing methods still largely depend on aryl and alkyl halides,[21−26] which can be expensive, difficult to prepare, or limited in functional group compatibility. We sought alternative cross-coupling partners and identified alkyl alcohols and aryl acids as promising candidates due to their commercial availability, structural diversity, and wide-ranging synthetic applicability.[27−30] Notably, aryl acids are an abundant class of reagents, yet their application in C(sp^3)–C(sp^2) coupling remains largely unexplored. While alcohols and aryl acids typically undergo esterification,[31] we sought to investigate whether a metallaphotoredox strategy[32] could facilitate the decarbonylative formation of C(sp^3)–C(sp^2) bonds (Figure 1a). In addition, aryl acids probe chemical space that is generally uncharted by aryl halides.[33] Therefore, this approach would offer complementary reactivity and expand access to a largely unexplored chemical space (Figure 1b).

Our group recently disclosed the use of a benzoxazolium salt (NHC) reagent to achieve the deoxygenation of alcohols under photoredox conditions,[34] enabling their selective activation in cross-coupling reactions.[35−37] In contrast, the metal-mediated activation of aryl acids has proven more challenging, typically requiring harsh reaction conditions and suffering from poor functional group tolerance.[38] The coupling of aryl carboxylic acids with aryl boron[39−43] or aryl halide[44,45] reagents is well-established, yet translating these techniques to the context of C(sp^2)–C(sp^3) bond formation has proven more difficult.

In recent, back-to-back publications, the Weix and Cernak groups have elegantly demonstrated nickel-catalyzed decarbonylation for C–C bond formation, highlighting the potential of aryl carboxylic acids to serve as versatile synthons in cross-coupling reactions.[33,46] Building on their work, we have integrated our group's alcohol deoxygenation strategy with this aryl acid activation approach to develop a system capable of efficiently forming C(sp^3)–C(sp^2) bonds with improved functional group tolerance. This combined method broadens the substrate scope, complementing existing cross-coupling

Received: November 8, 2024
Revised: April 9, 2025
Accepted: April 11, 2025
Published: April 23, 2025

ACS Publications
© 2025 American Chemical Society

https://doi.org/10.1021/jacs.4c15827
J. Am. Chem. Soc. 2025, 147, 14905–14914

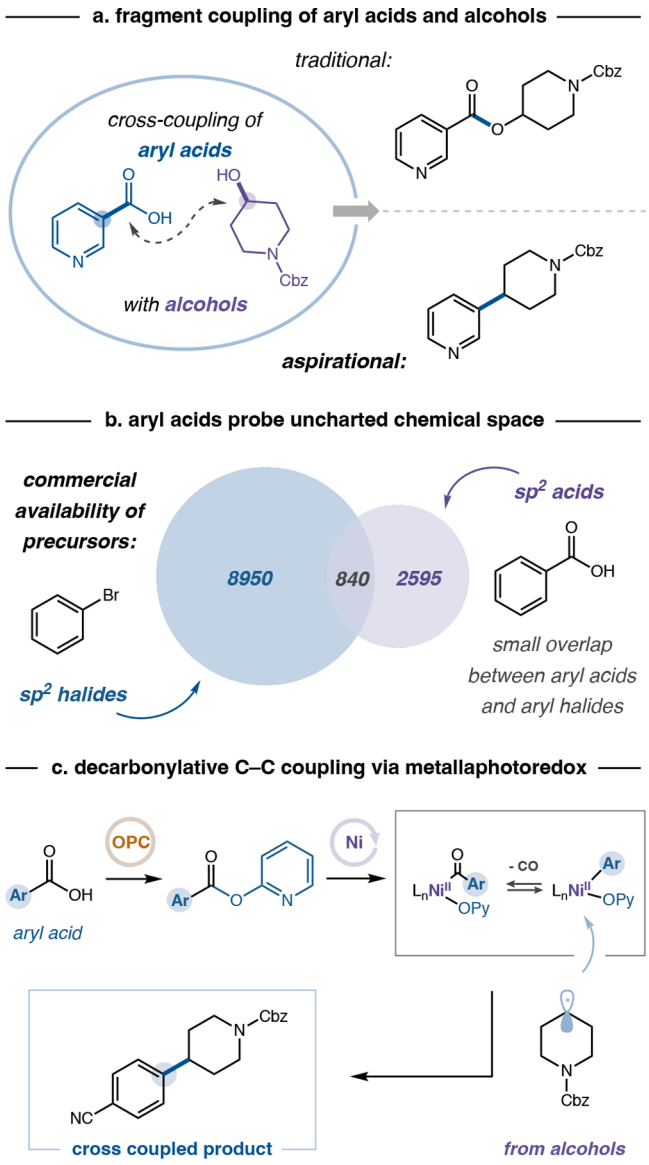

Figure 1. Cross-coupling of aryl acids and alkyl alcohols.

techniques and extending the reach of decarbonylative cross-coupling to new classes of compounds. Furthermore, this transformation provides an orthogonal strategy to traditional esterification, offering a novel pathway for the synthesis of complex molecular architectures (Figure 1c).

Herein, we demonstrate the broad applicability of our method across a wide array of alcohol and aryl acid coupling partners. Notably, the method operates fully at room temperature and exhibits excellent functional group tolerance, making it suitable for late-stage modification of pharmaceuticals and natural products. The versatility of this protocol, combined with its operational simplicity, makes it a valuable tool for synthetic chemists seeking to construct $C(sp^3)–C(sp^2)$ bonds from readily available starting materials.

We envisioned achieving dual nickel/photoredox-catalyzed cross-coupling of alcohols and aryl carboxylic acids according to the design plan depicted in Figure 2. Initially, aryl carboxylic acid **1** is premixed with dipyridin-2-yl carbonate (DPC) **2** and a catalytic amount of DMAP, resulting in the *in situ* formation of the activated acid **3** without purification.[47] In a separate reaction vessel, the alcohol substrate **4** reacts with NHC salt **5** to generate

Table 1. Optimized Conditions and Control Reactions[a]

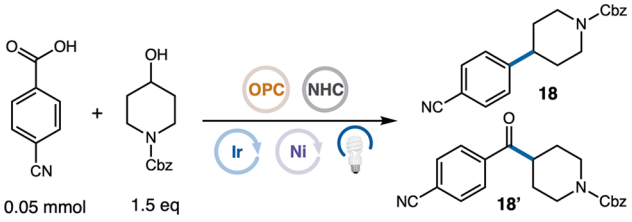

entry	deviation	yield[b] 18	yield[b] 18'
1	none	68%	12%
2	Cu^{I}-MFU-4l as CO scavenger	62%	8%
3	continuously sparge with N_2	67%	8%
4	no CO scavenger	39%	11%
5	no phthalimide	41%	33%
6	highest fan settings	43%	14%
7	0.05 M	36%	12%
8	5 mol% Ni, no phthalimide, no KOAc, no sieves	25%	62%
9	no photocatalyst	0%	0%
10	no Ni catalyst	0%	0%
11	isolated OPy ester	64%	10%

[a]**Acid activation:** acid (1.0 equiv), DMAP (1.0 mol %), dipyridin-2-yl carbonate (DPC) **2** (1.0 equiv). **Alcohol activation:** Alcohol (1.5 equiv), benzoxazolium salt (NHC-1) **5** (1.5 equiv), pyridine (1.5 equiv). **Reaction conditions**: $Ir[dF(CF_3)ppy]_2(dtbbpy)PF_6$ (2.0 mol %), Ni(4,4′-dMe-2,2′-bipyridine)Br_2 (15 mol %), quinuclidine "Q" (1.5 equiv), phthalimide (2.0 equiv), KOAc (2.0 equiv), 4 Å mol sieves (see the Supporting Information), 1:3 MTBE:t-Amyl OH (0.025 M), integrated photoreactor (450 nm, M2 plate, 50% light intensity), 16 h. [b]Yields determined by uHPLC analysis with mesitylene as standard.

the activated NHC–alcohol adduct **6** *in situ* under mildly basic conditions, also without further purification.[34] Upon visible-light excitation[48] of the photocatalyst $Ir[dF(CF_3)-ppy]_2(dtbbpy)PF_6$ (**7**), a long-lived oxidizing triplet excited state is generated (τ = 2.3 μs; $E_{1/2}^{red}$ [$*Ir^{III}/Ir^{II}$] = +1.21 V vs saturated calomel electrode (SCE) in MeCN).[49] This excited state complex **8** can undergo reductive quenching by the NHC–alcohol adduct **6** through single-electron transfer (SET), resulting in the formation of reduced Ir(II) photocatalyst **9**. Rapid deprotonation and subsequent β-scission of **10** leads to the liberation of an inert aromatized byproduct **12** and the generation of an alkyl radical **11**.[34] Concurrently, we hypothesized that the oxidative addition of Ni(0) species **13** into the activated acid would yield Ni(II) complex **14** which then undergoes decarbonylation to produce **15**. The alkyl radical can be quickly trapped by the nickel catalyst to form Ni(III)–alkyl intermediate **16**, which subsequently undergoes reductive elimination to form the desired cross-coupled product **18** while expelling Ni(I) intermediate **17**. Finally, SET between the Ir(II) species **9** and the Ni(I) complex **17** reduces Ni(I) to Ni(0) ($E_{1/2}^{red}$ [Ni^{II}/Ni^{0}] = −1.2 V versus SCE in DMF) and oxidizes Ir(II) ($E_{1/2}^{red}$ [Ir^{III}/Ir^{II}] = −1.37 V versus SCE in MeCN), thus simultaneously completing both the photoredox and nickel catalytic cycles.[50]

During our optimization campaign, a major challenge was minimizing the formation of the undesired ketone byproduct, which arises when the alcohol-derived alkyl radical is captured by the Ni(II) intermediate before productive decarbonylation. Initially, the ketone byproduct **18′** was formed in 62% yield

https://doi.org/10.1021/jacs.4c15827
J. Am. Chem. Soc. 2025, 147, 14905–14914

Table 2. Alkyl Alcohol and Alkyl Acid Scope[d]

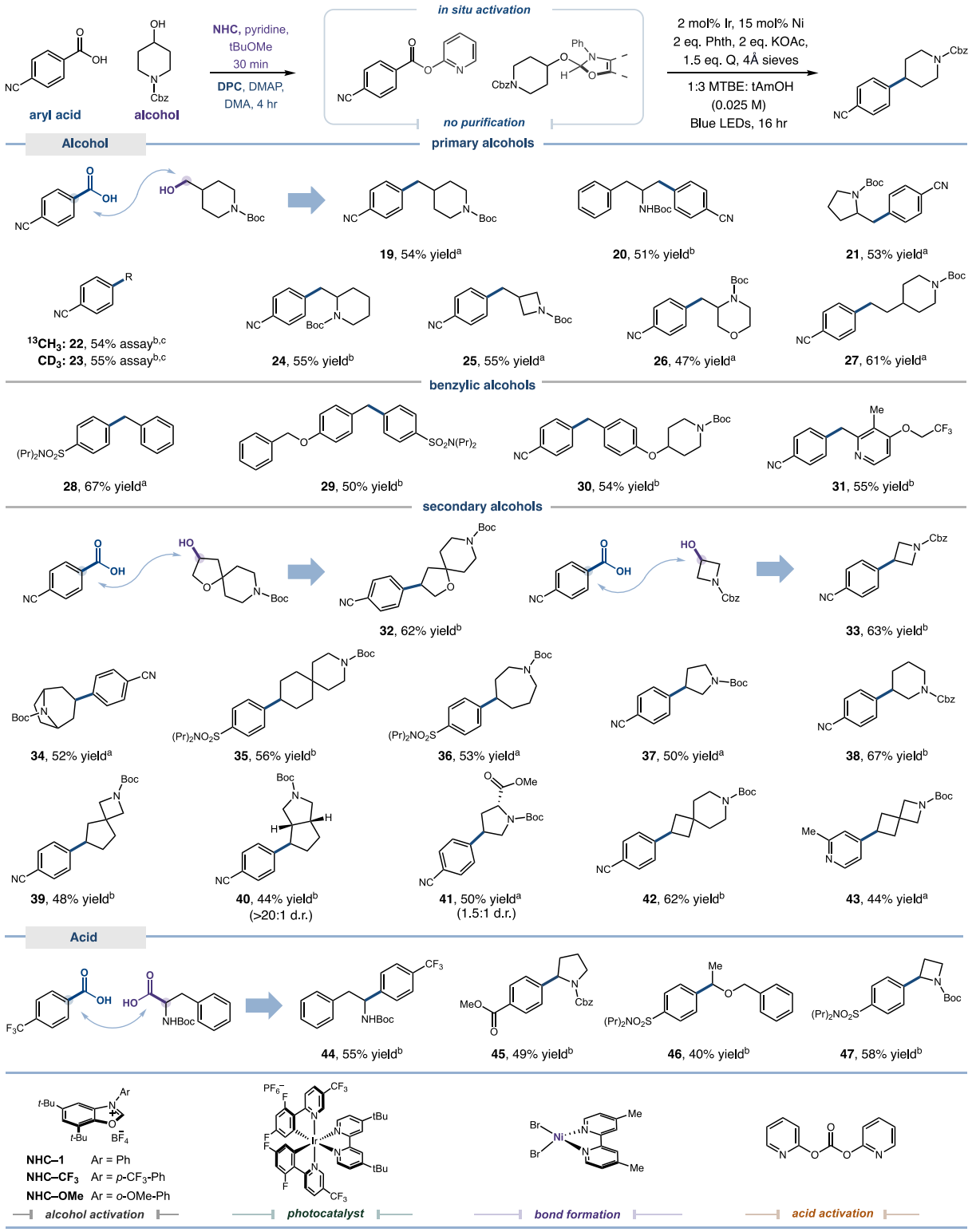

[a]Alcohol (1.5 equiv) aryl acid (1.0 equiv), Ir[dF(CF$_3$)ppy]$_2$(dtbbpy)PF$_6$ (2.0 mol %), Ni(4,4′-dMe-2,2′-bpy)Br$_2$ (15 mol %), NHC-1 **5** (1.5 equiv), pyridine (1.5 equiv), quinuclidine "Q" (1.5 equiv), phthalimide (2.0 equiv), KOAc (2.0 equiv), DMAP (1.0 mol %), DPC **2** (1.0 equiv), 4Å mol sieves (see the Supporting Information), 1:3 MTBE:t-Amyl OH (0.025 M), integrated photoreactor (450 nm, M2 plate), 16 h. [b]See the Supporting Information for experimental details. [c]Yield determined by uHPLC analysis. [d]Run at a 0.5 mmol scale. Yields are isolated unless specified.

(Table 1, entry 8). Mechanistic insights from the Weix lab indicate that both decarbonylation and oxidative addition are

https://doi.org/10.1021/jacs.4c15827
J. Am. Chem. Soc. 2025, 147, 14905−14914

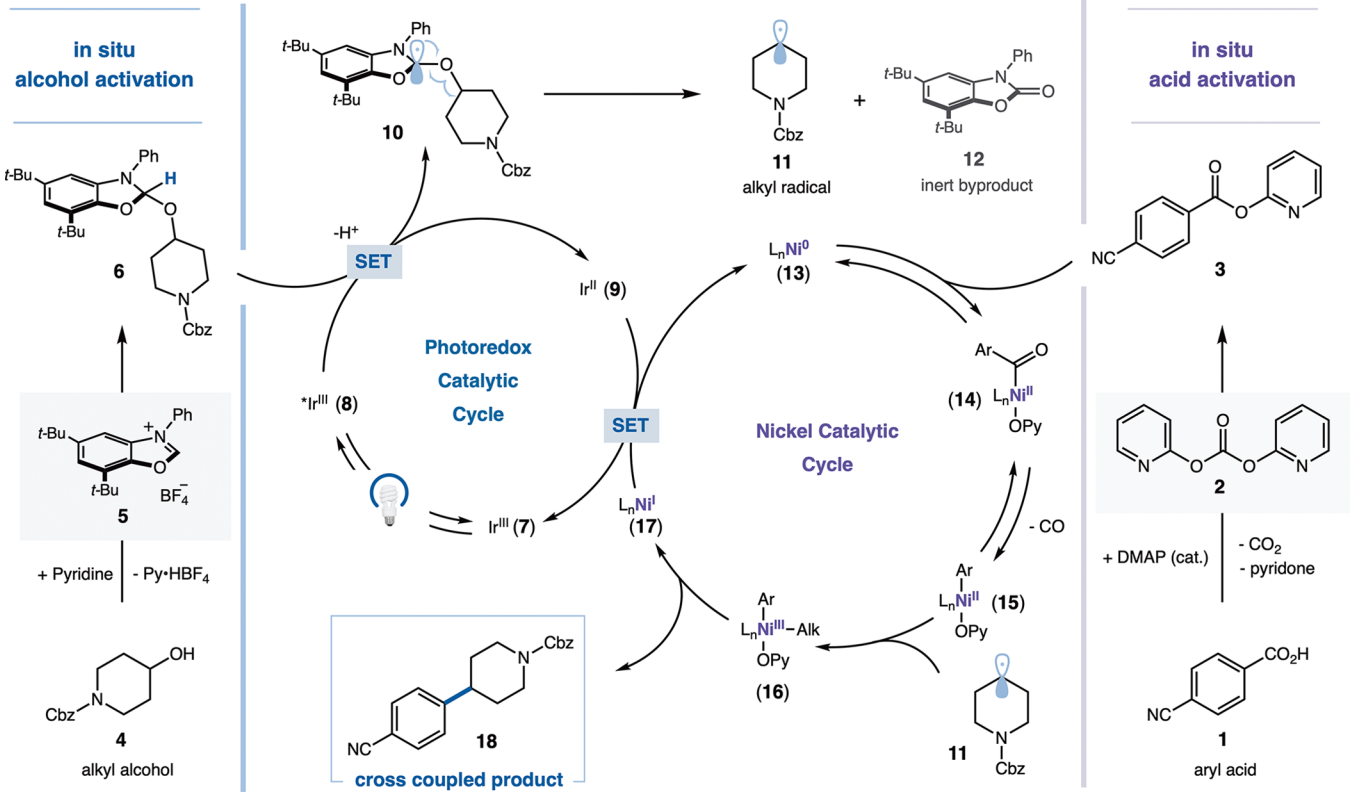

Figure 2. Proposed reaction mechanism.

rapid and reversible at room temperature.[46] Consequently, the efficient removal of CO from the system is critical, as the high affinity of Ni(0) for CO leads to undesired ketone formation.

Multiple strategies were deployed to address this challenge, which led to a reduction of ketone formation from 62% to 12% yield. These included the use of phthalimide, dilute reaction conditions, low fan settings on the integrated photoreactor, and CO scavengers such as 4 Å powdered molecular sieves or MOF CuI-MFU-4l.[51] Dilute reaction conditions and low fan settings helped to lower the CO concentration in the reaction mixture while increasing the reaction temperature, enhancing CO liberation from the nickel catalyst. Phthalimide likely discourages recarbonylation and stabilizes the Ni(II) complex through ligation, preventing unproductive Ni oligomerization or the formation of off-cycle Ni species.[52]

We found using 4 Å molecular sieves as a CO scavenger[53] as effective as nitrogen sparging (Table 1, entry 1 and 3), offering a more robust and user-friendly setup. Single-component CO adsorption isotherms for 4 Å molecular sieves reveal a modest isosteric enthalpy of adsorption of −25.6(1) kJ/mol (Figures S6 and S7). We hypothesize that during catalytic runs, CO is selectively sequestered via physisorption. Additionally, we observed that $Cu_{2.4}$-MFU-4l[51] ($Cu_{2.4}Zn_{2.6}Cl_{1.6}(btdd)_3$; H_2btdd = bis(1H-1,2,3-triazolo[4,5-*b*],[4′,5′-i])dibenzo[1,4]dioxin), a MOF containing trigonal pyramidal copper(I) sites that irreversibly scavenge CO at low partial pressures,[54] exhibits comparable performance to molecular sieves.

We were pleased to observe that under optimized conditions a broad range of primary and secondary alcohols were readily cross-coupled under the reaction conditions (Table 2; see the Supporting Information for optimization details). A variety of primary alcohols could be employed in this protocol in synthetically useful yields (**19**−**27**, 47−61% yield). The utility of this method is further demonstrated by the facile introduction of hydrogen- and carbon-enriched isotope units from commercial forms of methanol, obviating the need for lengthy de novo synthesis (**22** and **23**, 54% and 55% yield). Additionally, our studies revealed that primary benzylic alcohols were competent substrates, generating the desired products in good yield (**28**−**31**, 50−67% yield).

Secondary aliphatic alcohols were similarly effective in our protocol. Four-membered cyclic alcohols, such as azetidines (**33**, 63% yield) and strained azaspirocycles (**42** and **43**, 62% and 44% yield), performed well in this transformation. Five-membered cyclic alcohols containing saturated scaffolds of pharmaceutical relevance[55] were competent substrates, affording cross-coupled products incorporating pyrrolidine (**37**, 50% yield) and hydroxyproline (**41**, 50% yield). Additionally, five-membered spirocyclic and bicyclic ring systems bearing secondary alcohols could also be cross-coupled in good yield (**32**, **39**, and **40**, 44−62% yields). The method was extended to six-membered rings such as spirocyclic undecane systems (**35**, 56% yield) and piperidines (**38**, 67% yield). Azepanes were also efficiently coupled (**34** and **36**, 52% and 53% yields), showcasing the broad capability of this reaction to accommodate larger ring systems.

To further highlight the versatility of the method, we next extended our protocol beyond alcohols to include carboxylic acids as alkyl radical precursors.[56] Alkyl radicals were oxidatively generated from abundant feedstock α-amino acids—such as phenylalanine (**44**, 55% yield) and proline (**45**, 49% yield)—alongside an α-oxy acid (**46**, 40% yield) and noncanonical α-amino acid azetidine (**47**, 58% yield) en route to $C(sp^3)-C(sp^2)$ products.

We then explored the substrate scope of the reaction with respect to the aryl acid fragment (Table 3). A wide range of

https://doi.org/10.1021/jacs.4c15827
J. Am. Chem. Soc. 2025, 147, 14905−14914

Table 3. Aryl Acid Scope[d]

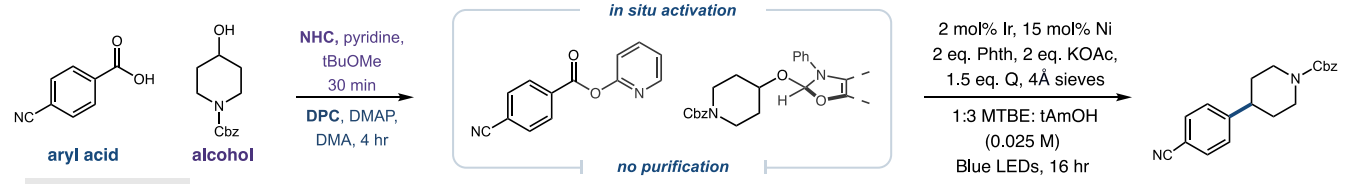

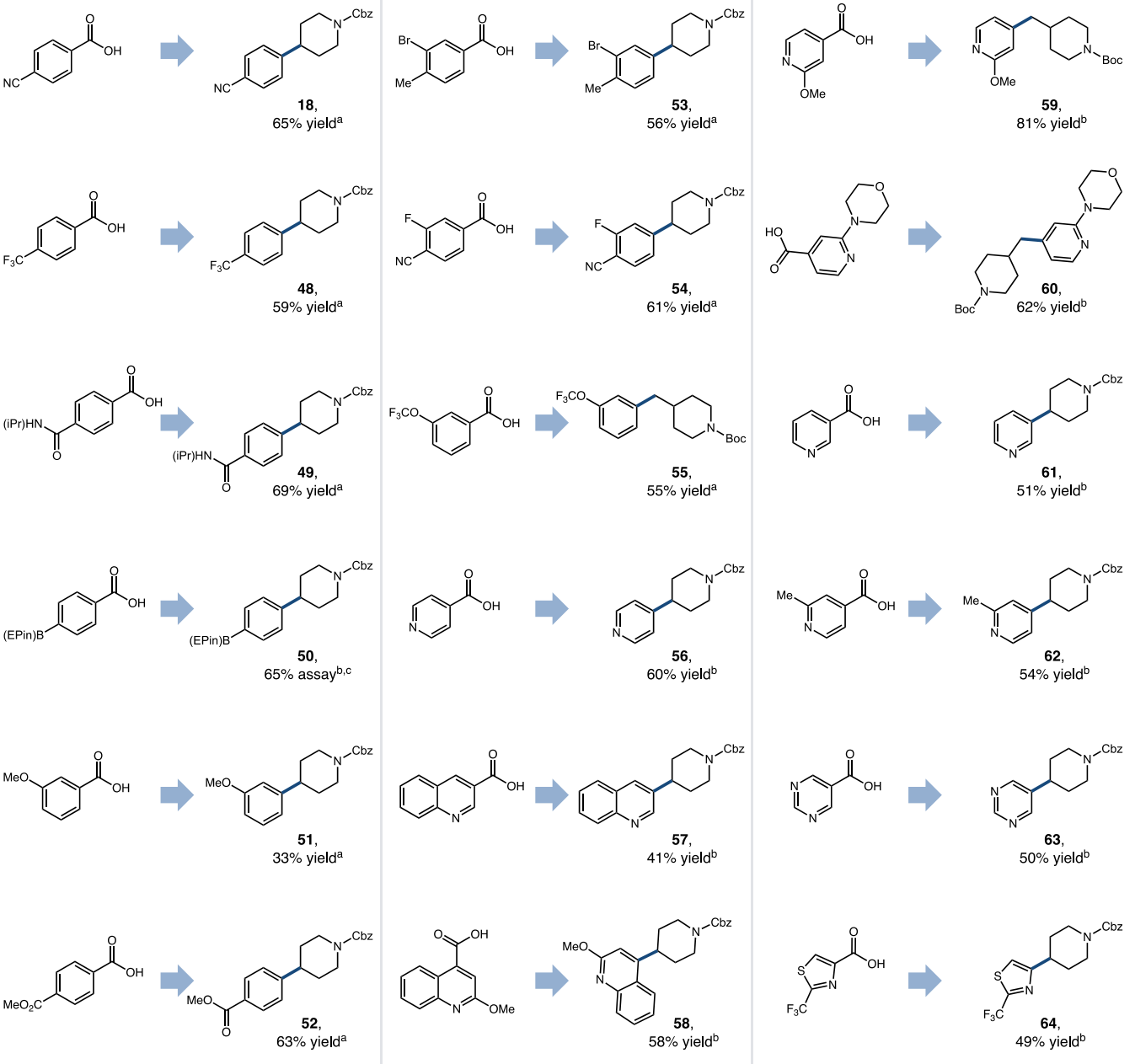

[a]Alcohol (1.5 equiv), acid (1.0 equiv), $Ir[dF(CF_3)ppy]_2(dtbbpy)PF_6$ (2.0 mol %), Ni(4,4′-dMe-2,2′-bipyridine)Br_2 (15 mol %), NHC-1 **5** (1.5 equiv), pyridine (1.5 equiv), quinuclidine "Q" (1.5 equiv), phthalimide (2.0 equiv), KOAc (2.0 equiv), DMAP (1.0 mol %), DPC **2** (1.0 equiv), 4Å mol sieves (see the Supporting Information), 1:3 MTBE:t-Amyl OH (0.025 M), integrated photoreactor (450 nm, M2 plate, 50% light intensity), 16 h. [b]See the Supporting Information for experimental details. [c]Yield determined by uHPLC. [d]Run at 0.5 mmol scale, and yields are isolated unless specified.

benzoic acids possessing diverse electronic and steric properties served as viable substrates (**18**, **48**−**55**, 33−69% yield). Excitingly, heteroaryl acids derived from pyridines, quinolines, and pyrimidines were also successfully coupled (**56**−**63**, 41−81% yield) as were five-membered heteroaryl acids such as thiazole (**64**, 49% yield). High functional-group compatibility was observed, with esters, ethers, nitriles, trifluoromethyl groups, aryl fluorides, aryl bromides, amines, benzyloxycarbonyl,

https://doi.org/10.1021/jacs.4c15827
J. Am. Chem. Soc. 2025, 147, 14905−14914

Table 4. Application to Late-Stage Functionalization of Biomolecules and Pharmaceuticals[d]

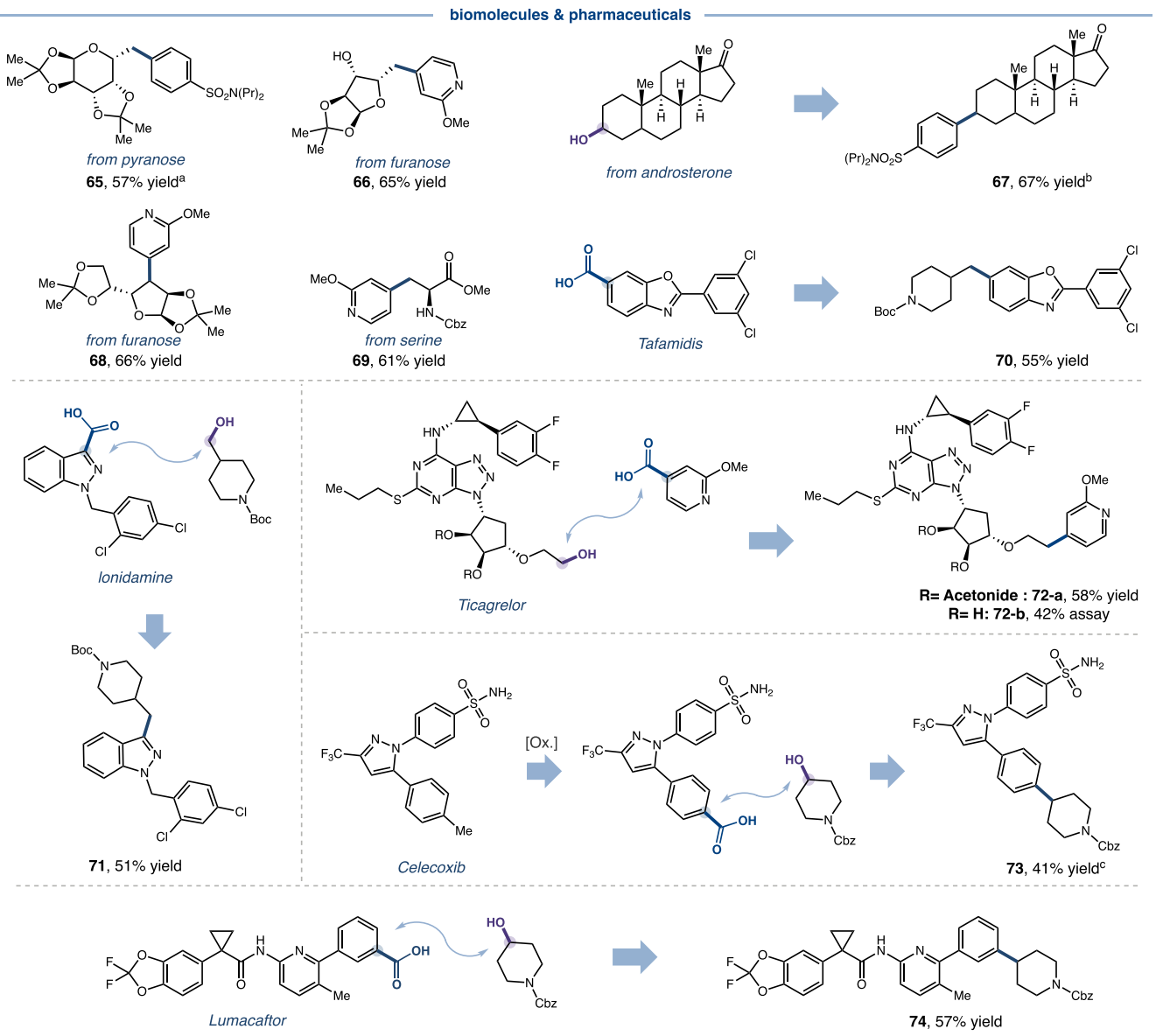

[a]>20:1 d.r. unassigned. [b]10:1 d.r. unassigned. [c]Yield given for the cross-coupling step only. [d]See the Supporting Information for experimental details. Run at 0.5 mmol scale, and all yields are isolated unless otherwise specified.

tert-butyl carbamate, and aryl boronic 1,1,2,2-tetraethylethylene glycol ester [B(EPin)] groups being well tolerated in the reaction. In line with previous findings,[33,46] electron-deficient acids favored C−C bond formation, likely due to more rapid decarbonylation, while electron-rich acids produced higher amounts of ketone byproducts, consistent with slower decarbonylation. Therefore, the reduced yields for more electron-rich acids (**51**, 33% yield) can be attributed to the slower oxidative addition of the 2-pyridyl ester to the Ni catalyst, along with diminished decarbonylation rates (Table S2).

Lastly, we sought to evaluate more complex alcohols and aryl acids for applications in late-stage functionalization. The wide availability of aryl carboxylic acids and alcohols facilitated the synthesis of products from diverse, complex starting materials. A range of pharmaceuticals were successfully deployed in the reaction, including tafamidis (**70**, 55% yield) and lonidamine (**71**, 51% yield)—both bearing valuable chloride functional groups—as well as lumacaftor (**74**, 57% yield) and ticagrelor (**72a,b**, 58% yield and 42% assay), were successfully employed in the reaction, forming the desired products in good yields. Additionally, saccharides (**65**, **66**, **68**, 57%, 65% and 66% yield), a derivative of canonical α-amino acid serine (**69**, 61% yield), and alcohol-bearing steroidal hormones such as androsterone (**67**, 67% yield) provided useful yields. Notably, in the case of furanose **66** and ticagrelor **72b**, exceptional regioselectivity was observed in which the primary alcohol was selectively targeted in the presence of secondary alcohols.

The utility of benzoic acids extends beyond their ready availability; these motifs offer significant synthetic versatility due to their ability to be masked as a variety of stable and accessible functional groups. For instance, tolyl groups in complex molecules such as celecoxib can be selectively oxidized to reveal aryl carboxylic acids. We envisioned applying this transformation in our cross-coupling protocol, allowing for the

https://doi.org/10.1021/jacs.4c15827
J. Am. Chem. Soc. 2025, 147, 14905−14914

modification of such intermediates to form a wide array of products.

This demethylative C−C cross-coupling strategy provides an efficient and flexible pathway to rapidly increase molecular complexity. As shown in Table 4, celecoxib-CO_2H, readily obtained upon benzylic oxidation of celecoxib, was subjected to the reaction conditions with benzyl 4-hydroxypiperidine-1-carboxylate to furnish the cross-coupled product in useful yields (**73**, 41% yield).

These results demonstrate the broad applicability of this strategy, particularly its tolerance for complex molecular structures, and the unique utility of aryl carboxylic acids as versatile building blocks in synthetic sequences. This versatility enables the efficient synthesis of valuable compound libraries, which can serve as pharmacophores or be subjected to further functionalization.[57] In addition, a commercial availability search revealed that 70% of the aryl carboxylic acids used in our scope were cheaper than their aryl bromide counterparts, in many cases by over an order of magnitude (Table S9). The approach underscores the potential for constructing complex molecular frameworks from abundant and easily accessible starting materials.

In conclusion, we present a formal cross-coupling of aryl carboxylic acids and alkyl alcohols to form $C(sp^3)$−$C(sp^2)$ bonds, offering not only a complementary strategy to conventional cross-coupling methods but also an orthogonal alternative to traditional esterification protocols. By combining NHC-mediated deoxygenation with nickel-mediated decarbonylative bond formation, we have developed a nickel/photoredox-catalyzed approach applicable to a broad range of aliphatic alcohols and aryl carboxylic acids. A key factor in the success of this transformation was the incorporation of molecular sieves and other scavengers to efficiently remove CO, thereby minimizing undesired ketone formation and enhancing reaction robustness. Using nontraditional cross-coupling partners, such as alcohols and aryl acids, this method enables access to novel $C(sp^3)$-rich chemical space. Overall, this aryl acid−alcohol coupling provides a versatile platform for expanding accessible chemical space.

■ ASSOCIATED CONTENT

Supporting Information

The Supporting Information is available free of charge at https://pubs.acs.org/doi/10.1021/jacs.4c15827.

Additional experimental details, optimization, additional substrate tables, characterization, and spectra (PDF)

■ AUTHOR INFORMATION

Corresponding Authors

Jeffrey R. Long − *Institute for Decarbonization Materials, Department of Chemistry, Department of Chemical and Biomolecular Engineering, and Department of Materials Science and Engineering, University of California, Berkeley, Berkeley, California 94720, United States; Materials Sciences Division, Lawrence Berkeley National Laboratory, Berkeley, California 94720, United States;* orcid.org/0000-0002-5324-1321; Email: jrlong@berkeley.edu

Chi "Chip" Le − *Department of Discovery Chemistry, Merck & Co., Inc., Boston, Massachusetts 02115, United States;* orcid.org/0000-0002-9614-365X; Email: chi.le@merck.com

David W.C. MacMillan − *Merck Center for Catalysis at Princeton University, Princeton, New Jersey 08544, United States;* orcid.org/0000-0001-6447-0587; Email: dmacmill@princeton.edu

Authors

Eva Lin − *Merck Center for Catalysis at Princeton University, Princeton, New Jersey 08544, United States*

Johnny Z. Wang − *Merck Center for Catalysis at Princeton University, Princeton, New Jersey 08544, United States;* orcid.org/0000-0001-5021-681X

Edna Mao − *Merck Center for Catalysis at Princeton University, Princeton, New Jersey 08544, United States*

Stephanie Tsang − *Department of Discovery Chemistry, Merck & Co., Inc., Boston, Massachusetts 02115, United States*

Kurtis M. Carsch − *Institute for Decarbonization Materials and Department of Chemistry, University of California, Berkeley, Berkeley, California 94720, United States;* orcid.org/0000-0003-4432-7518

Cesar N. Prieto Kullmer − *Merck Center for Catalysis at Princeton University, Princeton, New Jersey 08544, United States*

Ryan E. McNamee − *Merck Center for Catalysis at Princeton University, Princeton, New Jersey 08544, United States*

Complete contact information is available at: https://pubs.acs.org/10.1021/jacs.4c15827

Notes

The authors declare the following competing financial interest(s): D.W.C.M. declares a financial interest with respect to the Integrated Photoreactor.

■ ACKNOWLEDGMENTS

Research reported in this work was supported by the National Institute of General Medical Sciences of the National Institutes of Health (R35GM134897), the Princeton Catalysis Initiative, and Merck Sharp & Dohme LLC, a subsidiary of Merck & Co., Inc., Rahway, NJ, USA. The content is solely the responsibility of the authors and does not represent the official views of the NIGMS. E.L. acknowledges Princeton University for financial support through a first-year graduate fellowship. J.Z.W. acknowledges Princeton University, E. Taylor, and the Taylor family for an Edward C. Taylor Fellowship. E.M. thanks BMS for a Graduate Fellowship in Synthetic Organic Chemistry. K.M.C. is supported by an Arnold O. Beckman postdoctoral fellowship. Efforts to use metal−organic frameworks for the removal of CO were supported by the U.S. Department of Energy, Office of Basic Energy Sciences, Separation Science in the Chemical Sciences, Geosciences, and Biosciences Division, under Award Number DE- SC0019992.The authors thank the Roque Lab for generously allowing us to use their glovebox during the course of this work. We also thank V. Ciccone, P. Scott Pedersen and C. A. Gould for helpful scientific discussions and R. Lambert for assistance in preparing this manuscript.

■ REFERENCES

(1) (a) Lovering, F.; Bikker, J.; Humblet, C. Escape from Flatland: Increasing Saturation as an Approach to Improving Clinical Success. *J. Med. Chem.* **2009**, *52* (21), 6752−6756. (b) Lovering, F. Escape from Flatland 2: Complexity and Promiscuity. *Med. Chem. Commun.* **2013**, *4* (3), 515. (c) Lipinski, C.; Hopkins, A. Navigating Chemical Space for Biology and Medicine. *Nature* **2004**, *432*, 855−861.

(2) (a) Foley, D. J.; Craven, P. G. E.; Collins, P. M.; Doveston, R. G.; Aimon, A.; Talon, R.; Churcher, I.; von Delft, F.; Marsden, S. P.; Nelson, A. Synthesis and Demonstration of the Biological Relevance of sp^3-rich Scaffolds Distantly Related to Natural Product Frameworks. *Chem.—Eur. J.* **2017**, *23*, 15227−15232. (b) Singh, P. P.; Singh, P. K.; Srivastava, V. Visible Light Metallaphotoredox Catalysis in the Late-Stage Functionalization of Pharmaceutically Potent Compounds. *Org. Chem. Front.* **2022**, *10*, 216−236. (c) Cernak, T.; Dykstra, K. D.; Tyagarajan, S.; Vachal, P.; Krska, S. W. The Medicinal Chemist's Toolbox for Late Stage Functionalization of Drug-like Molecules. *Chem. Soc. Rev.* **2016**, *45*, 546−576. (d) Burke, M. D.; Schreiber, S. L. A Planning Strategy for Diversity-Oriented Synthesis. *Angew. Chem., Int. Ed.* **2004**, *43*, 46−58. (e) Ling, T.; Rivas, F. All- Carbon Quaternary Centers in Natural Products and Medicinal Chemistry: Recent Advances. *Tetrahredon* **2016**, *72*, 6729−6777. (f) Kranthikumar, R. Recent Advances in $C(sp^3)-C(sp^3)$ Cross- Coupling Chemistry: A Dominant Performance of Nickel Catalysts. *Organometallics* **2022**, *41* (6), 667−679. (g) Choi, J.; Fu, G. C. Transition Metal-Catalyzed Alkyl-Alkyl Bond Formation: Another Dimension in Cross-Coupling Chemistry. *Science* **2017**, *356* (6334), No. eaaf7230.

(3) (a) Togo, T.; Tram, L.; Denton, L. G.; ElHilali-Pollard, X.; Gu, J.; Jiang, J.; Liu, C.; Zhao, Y.; Zhao, Y.; Zheng, Y.; Zheng, Y.; Yang, J.; Fan, P.; Arkin, M. R.; Härmä, H.; Sun, D.; Canan, S. S.; Wheeler, S. E.; Renslo, A. R. Systematic study of Heteroarene stacking using a congeneric set of molecular glues for procaspase-6. *J. Med. Chem.* **2023**, *66* (14), 9784−9796. (b) Dougherty, D. A. Cation-π interactions involving aromatic amino acids. *J. Nutr.* **2007**, *137* (6), 1504S−1508S. (c) Liang, Z.; Li, Q. X. π−cation interactions in molecular recognition: Perspectives on Pharmaceuticals and Pesticides. *J. Agric. Food Chem.* **2018**, *66* (13), 3315−3323. (d) Bissantz, C.; Kuhn, B.; Stahl, M. A Medicinal Chemist's Guide to Molecular Interactions. *J. Med. Chem.* **2010**, *53* (14), 5061−5084.

(4) Lyon, W. L.; MacMillan, D. W. C. Expedient Access to Underexplored Chemical Space: Deoxygenative $C(sp^3)-C(sp^3)$ Cross-Coupling. *J. Am. Chem. Soc.* **2023**, *145*, 7736−7742.

(5) Campeau, L.-C.; Hazari, N. Cross- Coupling and Related Reactions: Connecting Past Success to the Development of New Reactions for the Future. *Organometallics* **2019**, *38*, 3−35.

(6) Johansson Seechurn, C. C. C.; Kitching, M. O.; Colacot, T. J.; Snieckus, V. Palladium-Catalyzed Cross-Coupling: A Historical Contextual Perspective to the 2010 Nobel Prize. *Angew. Chem., Int. Ed.* **2012**, *51*, 5062−5085.

(7) Buskes, M. J.; Blanco, M.-J. Impact of Cross-Coupling Reactions in Drug Discovery and Development. *Molecules* **2020**, *25*, 3493−3514.

(8) Haas, D.; Hammann, J. M.; Greiner, R.; Knochel, P. Recent Developments in Negishi Cross-Coupling Reactions. *ACS Catal.* **2016**, *6* (3), 1540−1552.

(9) Cordovilla, C.; Bartolomé, C.; Martínez-Ilarduya, J. M.; Espinet, P. The Stille Reaction, 38 Years Later. *ACS Catal.* **2015**, *5*, 3040−3053.

(10) Kambe, N.; Iwasaki, T.; Terao, J. Pd-Catalyzed Cross-Coupling Reactions of Alkyl Halides. *Chem. Soc. Rev.* **2011**, *40* (10), 4937−4947.

(11) Frisch, A. C.; Shaikh, N.; Zapf, A.; Beller, M. Palladium-Catalyzed Coupling of Alkyl Chlorides and Grignard Reagents. *Angew. Chem., Int. Ed.* **2002**, *41* (21), 4056−4059.

(12) Gagnon, A.; Albert, V.; Duplessis, M. Csp^3-Csp^2 Palladium-Catalyzed Cross-Coupling Reaction of Trialkylbismuth Reagents with Aryl, Heteroaryl, and Vinyl Halides and Triflates. *Synlett* **2010**, *2010* (19), 2936−2940.

(13) Roughley, S. D.; Jordan, A. M. The Medicinal Chemist's Toolbox: An Analysis of Reactions Used in the Pursuit of Drug Candidates. *J. Med. Chem.* **2011**, *54* (10), 3451−3479.

(14) Boström, J.; Brown, D. G.; Young, R.; Keserü, G. M. Expanding the medicinal chemistry synthetic toolbox. *Nat. Rev. Drug Discovery* **2018**, *17*, 709−727.

(15) Cooper, T. W. J.; Campbell, I. B.; Macdonald, S. J. F. Factors Determining the Selection of Organic Reactions by Medicinal Chemists and the Use of These Reactions in Arrays (Small Focused Libraries). *Angew. Chem., Int. Ed.* **2010**, *49*, 8082−8091.

(16) Schneider, N.; Lowe, D. M.; Sayle, R. A.; Tarselli, M. A.; Landrum, G. A. Big Data from Pharmaceutical Patents: A Computational Analysis of Medicinal Chemists' Bread and Butter. *J. Med. Chem.* **2016**, *59*, 4385−4402.

(17) Dombrowski, A. W.; Gesmundo, N. J.; Aguirre, A. L.; Sarris, K. A.; Young, J. M.; Bogdan, A. R.; Martin, M. C.; Gedeon, S.; Wang, Y. Expanding the Medicinal Chemist Toolbox: Comparing Seven $C(sp^2)$-$C(sp^3)$ Cross-Coupling Methods by Library Synthesis. *ACS Med. Chem. Lett.* **2020**, *11* (4), 597−604.

(18) Zhang, R.; Li, G.; Wismer, M.; Vachal, P.; Colletti, S. L.; Shi, Z. C. Profiling and Application of Photoredox $C(sp^3)$-$C(sp^2)$ Cross-Coupling in Medicinal Chemistry. *ACS Med. Chem. Lett.* **2018**, *9* (7), 773−777.

(19) Goldfogel, M. J.; Huang, L.; Weix, D. J. Cross-Electrophile Coupling: Principles and New Reactions. In *Nickel Catalysis in Organic Synthesis*; Ogoshi, S., Ed.; Wiley-VCH: Weinheim, 2020; pp 183−222.

(20) (a) Tellis, J. C.; Kelly, C. B.; Primer, D. N.; Jouffroy, M.; Patel, N. R.; Molander, G. A. Single-Electron Transmetalation via Photoredox/Nickel Dual Catalysis: Unlocking a New Paradigm for sp^3-sp^2 Cross-Coupling. *Acc. Chem. Res.* **2016**, *49* (7), 1429−1439. (b) Sakai, H. A.; Liu, W.; Le, C.; MacMillan, D. W. C. Cross-Electrophile Coupling of Unactivated Alkyl Chlorides. *J. Am. Chem. Soc.* **2020**, *142* (27), 11691−11697. (c) Zhang, P.; Le, C.; MacMillan, D. W. C. Silyl Radical Activation of Alkyl Halides in Metallaphotoredox Catalysis: A Unique Pathway for Cross-Electrophile Coupling. *J. Am. Chem. Soc.* **2016**, *138* (26), 8084−8087. (d) Hernández-Mejías, Á. D.; Shimozono, A. M.; Hazra, A.; Richter, S.; Tong, Z.; Langille, N. F.; Quasdorf, K.; Parsons, A. T.; Sigman, M. S.; Reisman, S. E. Ni-Catalyzed Enantioselective Desymmetrization: Development of Divergent Acyl and Decarbonylative Cross-Coupling Reactions. *J. Am. Chem. Soc.* **2025**, *147* (4), 3468−3477.

(21) Weix, D. J. Methods and Mechanisms for Cross-Electrophile Coupling of Csp^2 Halides with Alkyl Electrophiles. *Acc. Chem. Res.* **2015**, *48*, 1767−1775.

(22) Liu, J.; Ye, Y.; Sessler, J. L.; Gong, H. Cross-Electrophile Couplings of Activated and Sterically Hindered Halides and Alcohol Derivatives. *Acc. Chem. Res.* **2020**, *53*, 1833−1845.

(23) Hansen, E. C.; Li, C.; Yang, S.; Pedro, D.; Weix, D. J. Coupling of Challenging Heteroaryl Halides with Alkyl Halides via Nickel-Catalyzed Cross-Electrophile Coupling. *J. Org. Chem.* **2017**, *82* (14), 7085−7092.

(24) Noble, A.; McCarver, S. J.; Macmillan, D. W. C. Merging Photoredox and Nickel Catalysis: Decarboxylative Cross-Coupling of Carboxylic Acids with Vinyl Halides. *J. Am. Chem. Soc.* **2015**, *137* (2), 624−627.

(25) Chi, B. K.; Widness, J. K.; Gilbert, M. M.; Salgueiro, D. C.; Garcia, K. J.; Weix, D. J. In-Situ Bromination Enables Formal Cross-Electrophile Coupling of Alcohols with Aryl and Alkenyl Halides. *ACS Catal.* **2022**, *12* (1), 580−586.

(26) Kim, S.; Goldfogel, M. J.; Gilbert, M. M.; Weix, D. J. Nickel-Catalyzed Cross-Electrophile Coupling of Aryl Chlorides with Primary Alkyl Chlorides. *J. Am. Chem. Soc.* **2020**, *142* (22), 9902−9907.

(27) Wang, Y.; Haight, I.; Gupta, R.; Vasudevan, A. What Is in Our Kit? An Analysis of Building Blocks Used in Medicinal Chemistry Parallel Libraries. *J. Med. Chem.* **2021**, *64* (23), 17115−17122.

(28) Ertl, P. An Algorithm to Identify Functional Groups in Organic Molecules. *J. Cheminform* **2017**, *9* (1), 36.

(29) Ertl, P.; Schuhmann, T. A Systematic Cheminformatics Analysis of Functional Groups Occurring in Natural Products. *J. Nat. Prod.* **2019**, *82*, 1258−1263.

(30) Henkel, T.; Brunne, R. M.; Müller, H.; Reichel, F. Statistical Investigation into the Structural Complementarity of Natural Products and Synthetic Compounds. *Angew. Chem., Int. Ed.* **1999**, *38*, 643−647.

(31) Brown, D. G.; Boström, J. Analysis of Past and Present Synthetic Methodologies on Medicinal Chemistry: Where Have All the New Reactions Gone? *J. Med. Chem.* **2016**, *59*, 4443−4458.

(32) (a) Chan, A. Y.; Perry, I. B.; Bissonnette, N. B.; Buksh, B. F.; Edwards, G. A.; Frye, L. I.; Garry, O. L.; Lavagnino, M. N.; Li, B. X.; Liang, Y.; Mao, E.; Millet, A.; Oakley, J. V.; Reed, N. L.; Sakai, H. A.;

https://doi.org/10.1021/jacs.4c15827
J. Am. Chem. Soc. 2025, 147, 14905−14914

Seath, C. P.; MacMillan, D. W. C. Metallaphotoredox: The Merger of Photoredox and Transition Metal Catalysis. *Chem. Rev.* **2022**, *122* (2), 1485−1542. (b) Prier, C. K.; Rankic, D. A.; MacMillan, D. W. C. Visible Light Photoredox Catalysis with Transition Metal Complexes: Applications in Organic Synthesis. *Chem. Rev.* **2013**, *113*, 5322−5363. (c) Twilton, J.; Le, C. C.; Zhang, P.; Shaw, M. H.; Evans, R. W.; MacMillan, D. W. C. The Merger of Transition Metal and Photocatalysis. *Nat. Rev. Chem.* **2017**, *1*, 0052. (d) Skubi, K. L.; Blum, T. R.; Yoon, T. P. Dual Catalysis Strategies in Photochemical Synthesis. *Chem. Rev.* **2016**, *116*, 10035−10074. (e) Levin, M. D.; Kim, S.; Toste, F. D. Photoredox Catalysis Unlocks Single-Electron Elementary Steps in Transition Metal Catalyzed Cross-Coupling. *ACS Cent. Sci.* **2016**, *2*, 293−301.

(33) Douthwaite, J. L.; Zhao, R.; Shim, E.; Mahjour, B.; Zimmerman, P. M.; Cernak, T. Formal Cross-Coupling of Amines and Carboxylic Acids to Form sp^3−sp^2 Carbon−Carbon Bonds. *J. Am. Chem. Soc.* **2023**, *145* (20), 10930−10937.

(34) Dong, Z.; MacMillan, D. W. C. Metallaphotoredox-Enabled Deoxygenative Arylation of Alcohols. *Nature* **2021**, *598*, 451−456.

(35) (a) Sakai, H. A.; MacMillan, D. W. C. Nontraditional Fragment Couplings of Alcohols and Carboxylic Acids: C(sp^3)−C(sp^3) Cross-Coupling via Radical Sorting. *J. Am. Chem. Soc.* **2022**, *144*, 6185−6192. (b) Wang, J. Z.; Sakai, H. A.; MacMillan, D. W. C. Alcohols as Alkylating Agents: Photoredox-Catalyzed Conjugate Alkylation via In Situ Deoxygenation. *Angew. Chem., Int. Ed.* **2022**, *61*, No. e202207150. (c) Intermaggio, N. E.; Millet, A.; Davis, D. L.; MacMillan, D. W. C. Deoxytrifluoromethylation of Alcohols. *J. Am. Chem. Soc.* **2022**, *144*, 11961−11968. (d) Gould, C. A.; Pace, A. L.; MacMillan, D. W. C. Rapid and Modular Access to Quaternary Carbons from Tertiary Alcohols via Bimolecular Homolytic Substitution. *J. Am. Chem. Soc.* **2023**, *145*, 16330−16336. (e) Carson, W. P., II; Sarver, P. J.; Goudy, N. S.; MacMillan, D. W. C. Photoredox Catalysis-Enabled Sulfination of Alcohols and Bromides. *J. Am. Chem. Soc.* **2023**, *145*, 20767−20774. (f) Cai, Q.; McWhinnie, I. M.; Dow, N. W.; Chan, A. Y.; MacMillan, D. W. C Engaging Alkenes in Metallaphotoredox: A Triple Catalytic, Radical Sorting Approach to Olefin-Alcohol Cross-Coupling. *J. Am. Chem. Soc.* **2024**, *146* (18), 12300−12309. (g) Mao, E.; Prieto Kullmer, C. N.; Sakai, H. A.; MacMillan, D. W. C. Direct Bioisostere Replacement Enabled by Metallaphotoredox Deoxydifluoromethylation. *J. Am. Chem. Soc.* **2024**, *146* (8), 5067−5073. (h) Wang, J. Z.; Lyon, W. L.; MacMillan, D. W. C. Alkene Dialkylation by Triple Radical Sorting. *Nature* **2024**, *628* (8006), 104−109. (i) Chen, R.; Intermaggio, N. E.; Xie, J.; Rossi-Ashton, J. A.; Gould, C. A.; Martin, R. T.; Alcázar, J.; MacMillan, D. W. C. Alcohol-Alcohol Cross-Coupling Enabled by S_H2 Radical Sorting. *Science* **2024**, *383* (6689), 1350−1357.

(36) For select examples of alternative alcohol activation strategies for cross-coupling, see: (a) Zhang, X.; MacMillan, D. W. C. Alcohols as Latent Coupling Fragments for Metallaphotoredox Catalysis: sp3−sp2 Cross-Coupling of Oxalates with Aryl Halides. *J. Am. Chem. Soc.* **2016**, *138*, 13862−13865. (b) Vara, B. A.; Patel, N. R.; Molander, G. A. *O*-Benzyl Xanthate Esters under Ni/ Photoredox Dual Catalysis: Selective Radical Generation and Csp^3- Csp^2 Cross-Coupling. *ACS Catal.* **2017**, *7*, 3955−3959. (c) Suga, T.; Ukaji, Y. Nickel- Catalyzed Cross-Electrophile Coupling between Benzyl Alcohols and Aryl Halides Assisted by Titanium Co-reductant. *Org. Lett.* **2018**, *20*, 7846−7850.

(37) For select examples of other radical-based alcohol activation strategies, see: (a) Lackner, G. L.; Quasdorf, K. W.; Overman, L. E. Direct Construction of Quaternary Carbons from Tertiary Alcohols via Photoredox-Catalyzed Fragmentation of *tert*-Alkyl *N*-Phthalimidoyl Oxalates. *J. Am. Chem. Soc.* **2013**, *135*, 15342−15345. (b) Chenneberg, L.; Baralle, A.; Daniel, M.; Fensterbank, L.; Goddard, J.-P.; Ollivier, C. Visible Light Photocatalytic Reduction of *O*-Thiocarbamates: Development of a Tin-Free Barton-McCombie Deoxygenation Reaction. *Adv. Synth. Catal.* **2014**, *356*, 2756−2762. (c) Stache, E. E.; Ertel, A. B.; Rovis, T.; Doyle, A. G. Generation of Phosphoranyl Radicals via Photoredox Catalysis Enables Voltage-Independent Activation of Strong C−O Bonds. *ACS Catal.* **2018**, *8*, 11134−11139. (d) Nawrat, C. C.; Jamison, C. R.; Slutskyy, Y.; MacMillan, D. W. C.; Overman, L. E. Oxalates as Activating Groups for Alcohols in Visible Light Photoredox Catalysis: Formation of Quaternary Centers by Redox Neutral Fragment Coupling. *J. Am. Chem. Soc.* **2015**, *137*, 11270−11273. (e) Suga, T.; Takahashi, Y.; Miki, C.; Ukaji, Y. Direct and Unified Access to Carbon Radicals from Aliphatic Alcohols by Cost- Efficient Titanium-Mediated Homolytic C−OH Bond Cleavage. *Angew. Chem., Int. Ed.* **2022**, *61*, No. e202112533.

(38) Select examples of metal mediated aryl acid activation, see: (a) Gooßen, L. J.; Linder, C.; Rodríguez, N.; Lange, P. P.; Fromm, A. Silver-catalysed protodecarboxylation of carboxylic acids. *Chem. Commun.* **2009**, 7173−7175. (b) Gooßen, L. J.; Thiel, W. R.; Rodríguez, N.; Linder, C.; Melzer, B. Copper-Catalyzed Protodecarboxylation of Aromatic Carboxylic Acids. *Adv. Synth. Catal.* **2007**, *349*, 2241−2246. (c) Liu, X.; Jia, J.; Rueping, M. Nickel-Catalyzed C−O Bond Cleaving Alkylation of Esters: Direct Replacement of the Ester Moiety by Functionalized Alkyl Chains. *ACS Catal.* **2017**, *7*, 4491−4496. (d) Chatupheeraphat, A.; Liao, H.; Srimontree, W.; Guo, L.; Minenkov, Y.; Poater, A.; Cavallo, L.; Rueping, M. Ligand-Controlled Chemoselective C(acyl)−O Bond vs C(aryl)−C Bond Activation of Aromatic Esters in Nickel Catalyzed C(sp^2)−C(sp^3) Cross-Couplings. *J. Am. Chem. Soc.* **2018**, *140*, 3724−3735. (e) Masson-Makdissi, J.; Vandavasi, J. K.; Newman, S. G. Switchable Selectivity in the Pd-Catalyzed Alkylative Cross-Coupling of Esters. *Org. Lett.* **2018**, *20*, 4094−4098.

(39) (a) Muto, K.; Yamaguchi, J.; Musaev, D. G.; Itami, K. Decarbonylative organoboron cross-coupling of esters by nickel catalysis. *Nat. Commun.* **2015**, *6*, 7508−7515. (b) Malapit, C. A.; Bour, J. R.; Brigham, C. E.; Sanford, M. S. Base-Free Nickel-Catalysed Decarbonylative Suzuki−Miyaura Coupling of Acid Fluorides. *Nature* **2018**, *563* (7729), 100−104.

(40) Liu, C.; Ji, C.-L.; Qin, Z.-X.; Hong, X.; Szostak, M. Synthesis of Biaryls via Decarbonylative Palladium-Catalyzed Suzuki-Miyaura Cross-Coupling of Carboxylic Acids. *iScience* **2019**, *19*, 749−759.

(41) LaBerge, N. A.; Love, J. A. Nickel-Catalyzed Decarbonylative Coupling of Aryl Esters and Arylboronic Acids. *Eur. J. Org. Chem.* **2015**, *2015*, 5546−5553.

(42) Zhou, T.; Xie, P.; Ji, C.; Hong, X.; Szostak, M. Decarbonylative Suzuki−Miyaura Cross-Coupling of Aroyl Chlorides. *Org. Lett.* **2020**, *22*, 6434−6440.

(43) Dai, J.-J.; Liu, J.-H.; Luo, D.-F; Liu, L. Pd-catalysed decarboxylative Suzuki reactions and orthogonal O- arylation of aromatic carboxylic acids. *Chem. Commun.* **2011**, *47*, 677−679.

(44) Tang, J.; Biafora, A.; Goossen, L. J. Catalytic Decarboxylative Cross-Coupling of Aryl Chlorides and Benzoates without Activating ortho Substituents. *Angew. Chem., Int. Ed.* **2015**, *54*, 13130−13133.

(45) Gooßen, L. J.; Deng, G.; Levy, L. M. Synthesis of Biaryls via Catalytic Decarboxylative Coupling. *Science* **2006**, *313*, 662−664.

(46) Wang, J.; Ehehalt, L. E.; Huang, Z.; Beleh, O. M.; Guzei, I. A.; Weix, D. J. Formation of C(sp^2)−C(sp3) Bonds Instead of Amide C−N Bonds from Carboxylic Acid and Amine Substrate Pools by Decarbonylative Cross-Electrophile Coupling. *J. Am. Chem. Soc.* **2023**, *145* (18), 9951−9958.

(47) Beleh, O. M.; Alomari, S.; Weix, D. J. Synthesis of Stereodefined Enones from the Cross-Electrophile Coupling of Activated Acrylic Acids with Alkyl Bromides. *Org. Lett.* **2024**, *26* (34), 7217−7221.

(48) Le, C. C.; Wismer, M. K.; Shi, Z. C.; Zhang, R.; Conway, D. V.; Li, G.; Vachal, P.; Davies, I. W.; MacMillan, D. W. C. A General Small-Scale Reactor to Enable Standardization and Acceleration of Photocatalytic Reactions. *ACS Cent. Sci.* **2017**, *3*, 647−653.

(49) Lowry, M. S.; Goldsmith, J. I.; Slinker, J. D.; Rohl, R.; Pascal, R. A.; Malliaras, G. G.; Bernhard, S. Single-Layer Electroluminescent Devices and Photoinduced Hydrogen Production from an Ionic Iridium(III) Complex. *Chem. Mater.* **2005**, *17*, 5712−5719.

(50) Durandetti, M.; Nédélec, J.-Y.; Périchon, J. Nickel-Catalyzed Direct Electrochemical Cross-Coupling between Aryl Halides and Activated Alkyl Halides. *J. Org. Chem.* **1996**, *61* (5), 1748−1755.

(51) Carsch, K. M.; Huang, A. J.; Dods, M. N.; Parker, S. T.; Rohde, R. C.; Jiang, H. Z. H.; Yabuuchi, Y.; Karstens, S. L.; Kwon, H.; Chakraborty, R.; Bustillo, K. C.; Meihaus, K. R.; Furukawa, H.; Minor, A. M.; Head-Gordon, M.; Long, J. R. Selective Adsorption of

https://doi.org/10.1021/jacs.4c15827
J. Am. Chem. Soc. 2025, 147, 14905−14914

Oxygen from Humid Air in a Metal−Organic Framework with Trigonal Pyramidal Copper(I) Sites. *J. Am. Chem. Soc.* **2024**, *146* (5), 3160−3170.
(52) Prieto Kullmer, C. N.; Kautzky, J. A.; Krska, S. W.; Nowak, T.; Dreher, S. D.; MacMillan, D. W. C. Accelerating Reaction Generality and Mechanistic Insight through Additive Mapping. *Science* **2022**, *376* (6592), 532−539.
(53) Triebe, R. W.; Tezel, F. H. Adsorption of Nitrogen, Carbon Monoxide, Carbon Dioxide and Nitric Oxide on Molecular Sieves. *Gas Sep. Purif.* **1995**, *9* (4), 223−230.
(54) Denysenko, D.; Grzywa, M.; Tonigold, M.; Streppel, B.; Krkljus, I.; Hirscher, M.; Mugnaioli, E.; Kolb, U.; Hanss, J.; Volkmer, D. Elucidating Gating Effects for Hydrogen Sorption in MFU-4-Type Triazolate-Based Metal−Organic Frameworks Featuring Different Pore Sizes. *Chem. − Eur. J.* **2011**, *17* (6), 1837−1848.
(55) (a) Taylor, R. D.; MacCoss, M.; Lawson, A. D. G. Rings in Drugs. *J. Med. Chem.* **2014**, *57*, 5845−5859. (b) Vitaku, E.; Smith, D. T.; Njardarson, J. T. Analysis of the Structural Diversity, Substitution Patterns, and Frequency of Nitrogen Heterocycles among U.S. FDA Approved Pharmaceuticals. *J. Med. Chem.* **2014**, *57*, 10257−10274.
(56) For select examples of alkyl carboxylic acid activation via metallaphotoredox, see: (a) Zuo, Z.; MacMillan, D. W. C. Decarboxylative Arylation of α-Amino Acids via Photoredox Catalysis: A One-Step Conversion of Biomass to Drug Pharmacophore. *J. Am. Chem. Soc.* **2014**, *136*, 5257−5260. (b) Beil, S. B.; Chen, T. Q.; Intermaggio, N. E.; MacMillan, D. W. C. Carboxylic Acids as Adaptive Functional Groups in Metallaphotoredox Catalysis. *Acc. Chem. Res.* **2022**, *55*, 3481−3494. (c) Xuan, J.; Zhang, Z.-G.; Xiao, W.-J. Visible-Light-Induced Decarboxylative Functionalization of Carboxylic Acids and Their Derivatives. *Angew. Chem., Int. Ed.* **2015**, *54*, 15632−15641. (d) Schwarz, J.; König, B. Decarboxylative Reactions With and Without Light − A Comparison. *Green Chem.* **2018**, *20*, 323−361. (e) Johnston, C. P.; Smith, R. T.; Allmendinger, S.; MacMillan, D. W. C. Metallaphotoredox-Catalysed sp^3−sp^3 Cross-Coupling of Carboxylic Acids with Alkyl Halides. *Nature* **2016**, *536*, 322−325. (f) Kautzky, J. A.; Wang, T.; Evans, R. W.; MacMillan, D. W. C. Decarboxylative Trifluoromethylation of Aliphatic Carboxylic Acids. *J. Am. Chem. Soc.* **2018**, *140*, 6522−6526. (g) Liang, Y.; Zhang, X.; MacMillan, D. W. C. Decarboxylative sp^3 C−N Coupling via Dual Copper and Photoredox Catalysis. *Nature* **2018**, *559*, 83−88. (h) Zhao, W.; Wurz, R. P.; Peters, J. C.; Fu, G. C. Photoinduced, Copper-Catalyzed Decarboxylative C−N Coupling to Generate Protected Amines: An Alternative to the Curtius Rearrangement. *J. Am. Chem. Soc.* **2017**, *139*, 12153−12156. (i) Mao, R.; Frey, A.; Balon, J.; Hu, X. Decarboxylative C(sp^3)−N cross-coupling via synergetic photoredox and copper catalysis. *Nat. Catal.* **2018**, *1*, 120−126.
(57) Kutchukian, P. S.; Dropinski, J. F.; Dykstra, K. D.; Li, B.; DiRocco, D. A.; Streckfuss, E. C.; Campeau, L.-C.; Cernak, T.; Vachal, P.; Davies, I. W.; Krska, S. W.; Dreher, S. D. Chemistry Informer Libraries: A Chemoinformatics Enabled Approach to Evaluate and Advance Synthetic Methods. *Chem. Sci.* **2016**, *7* (4), 2604−2613.

https://doi.org/10.1021/jacs.4c15827
J. Am. Chem. Soc. 2025, 147, 14905−14914